

Radiative heating of plastic-tamped aluminum foil by x rays from a foam-buffered hohlraum

Jiyan Zhang,¹ Jiamin Yang,¹ Yan Xu,² Guohong Yang,¹ Yaonan Ding,¹ Jun Yan,² Jianmin Yuan,³ Yongkun Ding,¹ Zhijian Zheng,¹ Yang Zhao,¹ and Zhimin Hu¹

¹Research Center of Laser Fusion, P. O. Box 919-986, Mianyang 621900, China

²Institute of Applied Physics and Computational Mathematics, Beijing 100088, China

³National University of Defense Technology of China, Changsha 410073, China

(Received 18 July 2008; revised manuscript received 20 October 2008; published 7 January 2009)

The time dependence of the x-ray absorption of aluminum samples heated with intense radiation sources from a foam-buffered gold hohlraum has been studied in this work. Hydrodynamic simulations were used to illustrate the plasma conditions in the plastic-tamped aluminum foils contained in this type of hohlraum. Experiments were conducted to measure the *K*-shell x-ray absorption spectra of the aluminum sample. With densities taken from the hydrodynamic simulations, electron temperatures were then inferred by fitting the measured absorption spectra with detailed-term-accounting calculations. The inferred temperatures have a maximum of about 93 eV and were found to agree within 25% with the simulated results at times after 1 ns, indicating that the use of foam shields, together with a compact cavity, has created a clean and high-temperature radiation source preferable to opacity measurements.

DOI: 10.1103/PhysRevE.79.016401

PACS number(s): 52.25.Os, 52.70.La

I. INTRODUCTION

The x-ray absorption properties of hot dense plasma are of great interest in high-energy-density physics applications such as inertial confinement fusion and laboratory astrophysics [1,2]. Currently, most opacity data used in physical applications are generated using theoretical models. These theoretical models for computing opacity are complex and rely on various approximations [3–5]. In order to test and improve these models, it is necessary to perform laboratory measurements of x-ray opacities of well-characterized plasma samples.

Experimental measurements of x-ray opacities of hot dense plasmas have long been a great challenge to researchers in high-energy-density physics, especially at temperature as high as occur in stellar interiors, since they often need more energy and the backlight must be bright enough to overwhelm the sample self-emission. With the development of high-power pulse machines such as the laser and Z pinch, great progress has been made in laboratory measurements of opacity. In high-power laser facilities, a series of opacity experiments have been carried out [6–16]. In some of these experiments, high-quality opacity data were obtained, with the plasma conditions, i.e., the temperature and density of the sample, being measured simultaneously and independently [6–13]. The typical sample temperatures achieved in these laser-based opacity experiments are below 70 eV. On the most powerful Z pinch facility at Sandia National Laboratory, opacity samples have recently been heated up to temperatures above 150 eV [17–19]. However, the density and temperature of the samples in these Z-pinch-based experiments were not determined independently and relied on hydrodynamic simulations, so that this kind of opacity measurement cannot be considered as an exact one. In fact, almost all the exact opacity measurements have been carried out in laser facilities, though at relatively low sample temperatures. One of the greatest difficulties that prevents us from measuring the opacity at high temperature is that a

smaller hohlraum has to be used to generate a higher radiation temperature when the total laser energy is limited, while with a smaller hohlraum, it would be more difficult to prevent the stray laser light from irradiating the sample, or the blow-off plasmas from colliding with the sample plasma.

Recently, with an improved target design, we carried out experimental measurements of the *K*-shell absorption spectra of aluminum plasmas on SG-II laser facilities with a foam-buffered hohlraum [20], i.e., a hohlraum with foam shields to isolate the laser-produced gold plasmas and the sample. By fitting the aluminum transmission with theoretical calculations from a combination of radiative hydrodynamics simulations and atomic physics code, a maximum temperature of about 95 eV was found in the aluminum sample. In this paper, we will report in detail on the time-dependent plasma temperatures in an aluminum sample radiatively heated by radiation from a foam-buffered hohlraum. We will perform radiative hydrodynamics calculation to simulate the temperature evolution in the radiatively heated sample, and we will also perform experimental measurements of the sample temperatures by fitting the experimental absorption spectra with detailed-term-accounting calculations, with the delay times of the backlight varied to sample the temperature at different times after sample heating starts. We will prove that such a hohlraum design can indeed be used to obtain high-quality x-ray absorption spectrum of a high-temperature sample with a less powerful laser facility. In fact, the main purpose of this work is more to provide meaningful data to test our target designs than to obtain quantitative opacity data.

II. EXPERIMENTAL MEASUREMENTS

The sample in an opacity experiment is often placed in the center of a gold cylindrical hohlraum. When laser beams are injected into the hohlraum, high-temperature gold plasmas are produced and blow from the hohlraum wall. These gold plasmas efficiently convert the laser energy into x-ray radiation and build a high-temperature radiation field in the hohl-

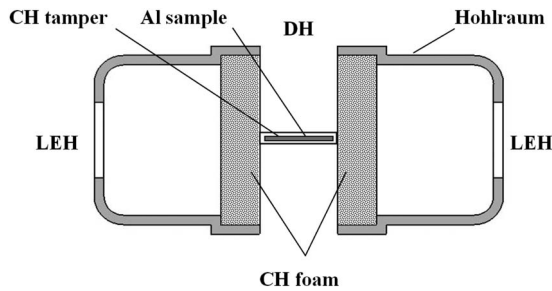


FIG. 1. Target geometry employed in the experiment and simulation. Note that the diagnostic holes (DHs) on the target are used for spectral measurement.

raum. The blow-off from the walls may collide with the sample plasma, and its emission may disturb the opacity measurement. Furthermore, stray laser light from the laser-produced plasmas may hit the sample and drive the sample out of local thermodynamic equilibrium (LTE). In some early experiments, baffles were suggested to prevent the sample from being irradiated by the laser light and blow-off plasmas and were proved a success in opacity measurements. However, the existence of baffles limits the hohlraum to a relatively large size, thus resulting in a relatively low radiative temperature in the hohlraum. Instead of using baffles, we use foam shields to isolate the sample and the laser-irradiated walls. Shown in Fig. 1 is the target geometry used in the experiment. By placing two slices of foam plates with appropriate areal density between the sample and the laser-irradiated walls, it is possible to let the x-ray radiation pass by with lower energy loss and at the same time prevent any blow-off plasmas and stray laser light from hitting the sample plasma. The use of foam shields has made it possible for us to design an opacity target more compact and consequently with higher radiative temperature.

The experimental setup is shown in Fig. 2. Eight main beams of the SG-II laser, arranged in cones on either side of a gold cylindrical hohlraum so that each beam forms an angle of 45° to the hohlraum axis, enter the hohlraum at both ends through laser entrance holes (LEHs) of 380 μm diameter. The beams cross at the center of the holes and are diverging so that they produce an elliptical spot on the hohlraum wall of about 400 × 300 μm² size. The laser light is frequency tripled and has a total energy of 2 kJ and pulse duration of 1 ns. Two slices of plastic carbon-hydrogen (CH)

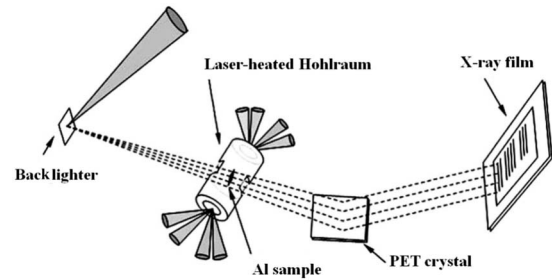


FIG. 2. Experimental setup.

foam of $\phi 780 \mu\text{m}$ in diameter and $200 \mu\text{m}$ in thickness were placed between the sample and the laser-irradiated hohlraum walls. The density of the foam is about 40 mg/cm^3 and is larger than the critical density of CH plasma for a $0.35 \mu\text{m}$ laser, that is, 32.5 mg/cm^3 , thus being able to prevent effectively the stray laser light from hitting the aluminum sample. The temporal behavior of the radiation was monitored by a soft x-ray spectrometer (SXS) from the laser entrance hole at an angle of 30° relative to the hohlraum axis. The soft x-ray spectrometer is a combination of an array of seven channel-filtered x-ray diodes array coupled to oscillographs and covers an x-ray energy range of about 50–1500 eV. The simulated radiation temperature and the radiation temperature inferred from the SXS data for the six shots are illustrated in Fig. 3(a). It is found that the measured radiation temperatures match the simulations quite well. A $40 \mu\text{g/cm}^2$ aluminum foil is placed in the center of the hohlraum and heated volumetrically by x-ray radiation passing through the foam shields. The aluminum sample is sandwiched between two $150 \mu\text{g/cm}^2$ layers of plastic, which help reduce the axial density gradients and improve the homogeneity of the heated sample. The frequency-doubled ninth laser beam, carrying energy of about 200 J in a 130 ps Gaussian pulse, is focused by an $f/4.5$ lens onto a gold disk with an incidence angle of 45° (the size of the focal spot being about $100 \mu\text{m}$). The gold disk is placed at a distance of $2500 \mu\text{m}$ from the sample plane and the laser-produced gold plasma provides the necessary short-pulse point-projection backlight for absorption measurements.

The point-projection-spectroscopy geometry is used to measure the absorption spectra of the radiatively heated aluminum foil, but the backlight, sample emission, and sample absorption are recorded on separate shots to minimize the

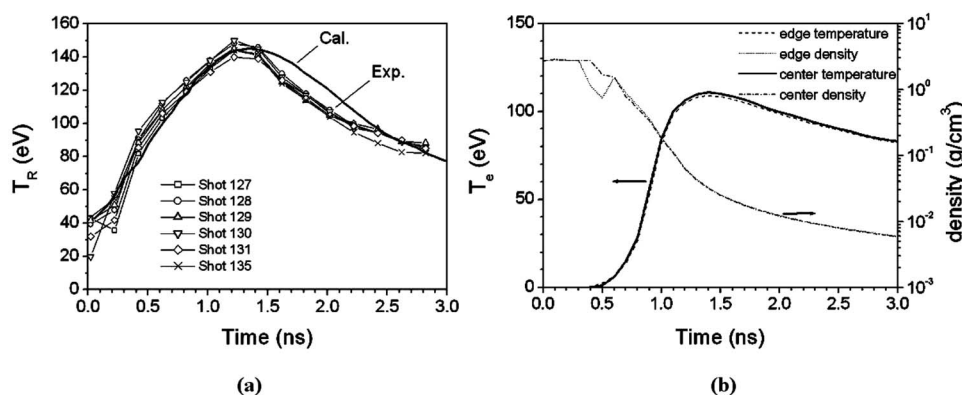


FIG. 3. (a) Time behavior of the radiation temperatures measured by SXS from an angle 30° relative to the hohlraum axis (lines with symbols) and the simulations (solid line), with the measured temperatures in different shots labeled by different symbols. (b) Simulated evolution of the density and temperature in the radiatively heated CH-tamped aluminum sample with the measured radiation source shown in (a).

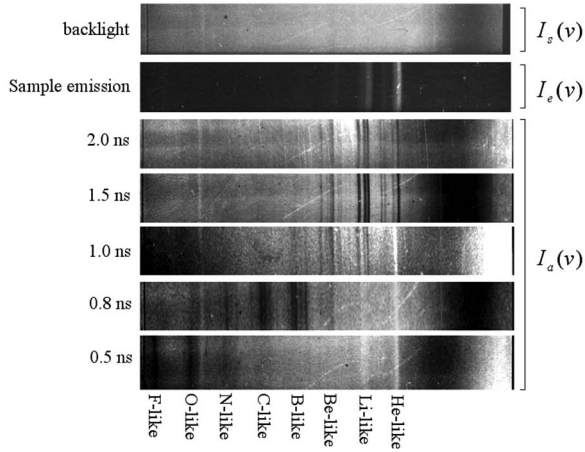


FIG. 4. Film data of the backlight spectrum, sample self-emission spectrum, and absorption spectra measured at five delay times of 0.5, 0.8, 1.0, 1.5, and 2.0 ns.

effects of the finite source size, since the diameter of the backlight source is relatively large compared to the width of the sample, which limits the spatial resolution of the measuring system and makes it difficult to measure the backlight, sample emission, and sample absorption simultaneously in one shot. The measurement of the absorption spectra is time resolved, with the temporal resolution of the measurement determined by the duration of the x-ray backlight source, which was measured by x-ray streak camera to have a duration of about 200 ps. By variation of the delay time of the backlight related to the main heating beams, the absorption spectra can be sampled at a series of times after sample heating starts up. Figure 4 shows the spectra obtained on seven separate shots. The x rays passing through the CH-tamped aluminum foil, that is, the backlight attenuated by both aluminum and CH layers, is measured with a pentaerythritol (PET) crystal spectrometer on five separate shots with delay times of 0.5 ns (shot 131), 0.8 ns (shot 135), 1.0 ns (shot 130), 1.5 ns (shot 127), and 2.0 ns (shot 129). These spectra give the *K*-shell absorption of the aluminum plasma and illustrate that the absorbers shift from F-like to He-like ions as the sample heating goes on. The x rays passing through only the CH layers are measured on another shot and give the backlight spectrum. The sample emission is also measured on a separate shot.

The film optical density was measured versus position using a film scanner that has been rectified to a microdensitometer. The scanned data were converted from optical density to x-ray exposure by the results of the premeasured response properties of the film. Energy calibration was performed using the *K*-shell emission line of the aluminum plasma. The background contributions from the chemical fog and the x-ray fluorescence were determined from the section of the film that was not exposed to x rays from the backlight and the sample, but was exposed to the fluorescence from the spectrometer. These background signals were then subtracted from both the absorption signal and the source signal. With the backgrounds subtracted, the plasma transmission was then obtained by comparing the direct and attenuated x-ray signals. Note here that the absorption contributions from the

CH foil in the separate shots are approximately the same and can be eliminated in deducing the aluminum transmission.

The sample transmissions were obtained by a procedure similar to that described in the literature [9], except that the CH layers were also included in the present treatment. Assuming that τ^{Al} and τ^{CH} are the optical depths of the aluminum sample and the CH tamper, the intensity information recorded on the separate shots can be written respectively as

$$I_a(v) = I_0(v)\exp[-\tau^{\text{Al}}(v) - \tau^{\text{CH}}(v)] + I_e^0(v) + I_{\text{fog}} + I_{\text{fluorescence}}, \quad (1)$$

$$I_s(v) = I_0(v)\exp[-\tau^{\text{CH}}(v)] + I_{\text{fog}} + I_{\text{fluorescence}}, \quad (2)$$

$$I_e(v) = I_e^0(v) + I_{\text{fog}} + I_{\text{fluorescence}}, \quad (3)$$

where $I_e^0(v)$ is the sample emission intensity, $I_0(v)$ is the backlight source intensity, I_{fog} is the film fog, and $I_{\text{fluorescence}}$ is the spectrometer fluorescence. From Eqs. (1)–(3), the aluminum transmission can be obtained as

$$T(v) = \exp[-\tau^{\text{Al}}(v)] = \frac{I_a(v) - I_e(v)}{I_s(v) - I_{\text{fog}} - I_{\text{fluorescence}}}. \quad (4)$$

Note in Eq. (4) that the CH emission is neglected since it has little contribution to the film intensity in the measured wavelength range.

The optical thickness $\tau(v)$ is usually defined as

$$\tau(v) = \int_0^L \mu(v, x)\rho(x)dx, \quad (5)$$

where $\rho(x)$ is the density and $\mu(v, x)$ is the opacity at x in the sample, and L is the sample thickness. For a uniform sample

$$\tau(v) = \mu(v)\rho L, \quad (6)$$

it is well known that an optical thin foil expands approximately one-dimensionally when it is subjected to intense radiation, which means that the sample areal density remains almost unchanged during the heating process and is determined uniquely by its initial areal density.

III. HYDRODYNAMIC SIMULATIONS

In this work, hydrodynamics codes were used to simulate the evolution of the radiatively heated sample in the foam-buffered hohlraum. The target used in the simulations, as described in Sec. II, is in fact a cylindrical gold cavity containing two slices of low-density CH foam shields and a CH-tamped aluminum sample, with the foam shields placed between the laser-produced plasma and the tamped sample. The foam shields have just the same role as the baffles in the target designed by Perry *et al.* [8,9]. However, the foam shields have the advantage of using a more compact hohlraum and consequently obtaining a higher radiation temperature in it. As was discussed in [21–23], the relatively low heat capacity of the low-density foam makes it possible for radiation to pass through supersonically with less energy loss. In this work, the thickness and density of the foam are not the optimum ones. They are chosen so as to facilitate the

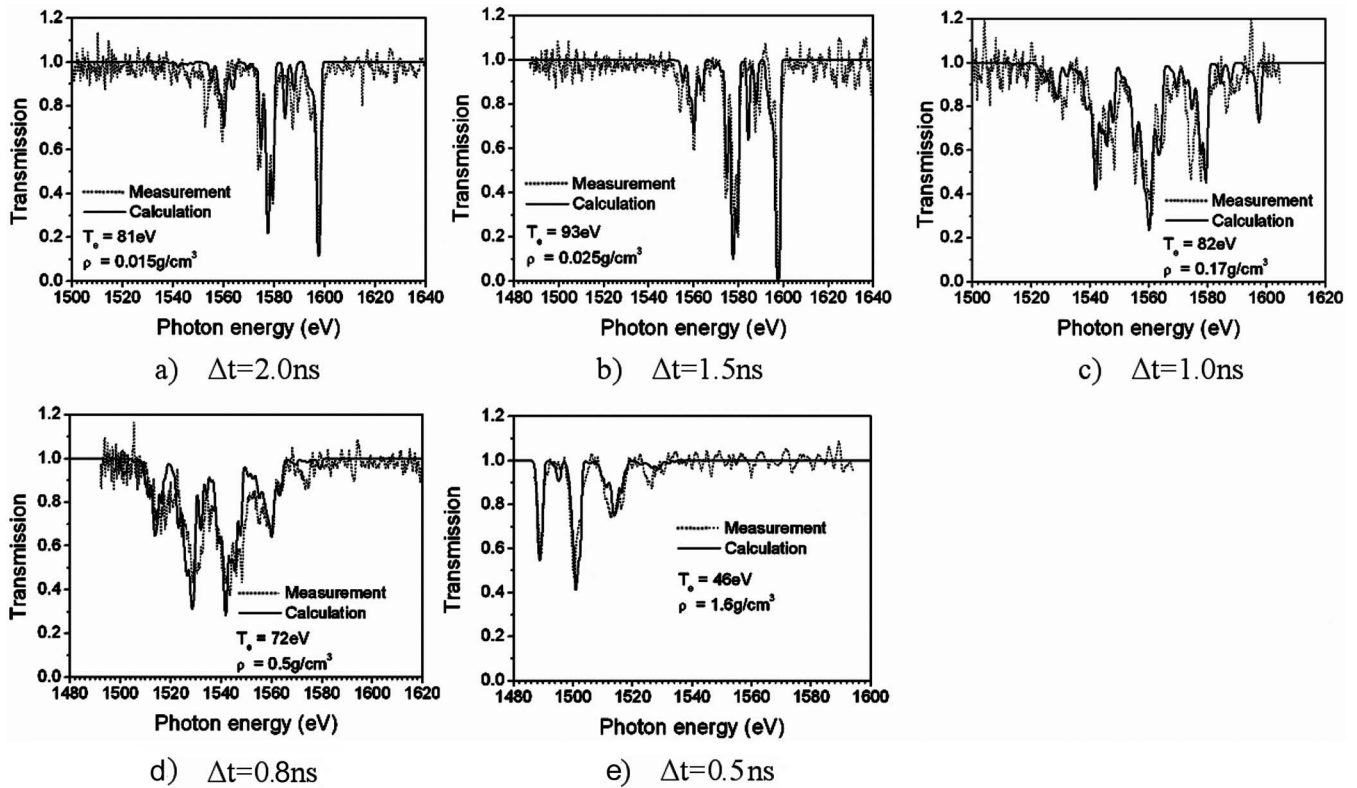


FIG. 5. Comparison between the measured and calculated transmission in radiatively heated aluminum foils. The calculations are shown as solid lines, while the measurements are shown as dotted lines. In the calculations, the densities are obtained from hydrodynamic simulations while the temperatures are deduced from the best fits of the experimental transmission.

machining of the foam, though smaller thickness and lower density should have been used.

With the measured x-ray source, hydrodynamic simulations have been performed to infer the plasma conditions. Several codes were used in the simulations. First, a three-dimensional x-ray Monte Carlo transfer code RT3D was used to simulate the redistribution of x-ray radiation in the hohlraum. Second, the radiation passing through the 200 μm CH foam plate of density 40 mg/cm^3 was simulated using the two-dimensional multigroup transport code LARED-R-1. Third, again the code RT3D is used to simulate the redistribution of radiation passing through the 200 μm CH foam plate on the sample. The calculated radiation reaching the sample surface is used as input to the next step. Finally, a one-dimensional multigroup transport code RDMG is used to simulate the hydrodynamic expansion of the sample, with the radiation on the sample calculated using RT3D. Figure 3(b) shows the evolution of the sample density and temperature at two points in the sample. The two positions represent, respectively, the edge and the center of the sample, where the term “edge” means the surface of the Al sample foil. The plots show that the temperature in the sample rises to a maximum of 110 eV at 1.0 ns after the laser impinged on the target and that there are only small temperature gradients in the sample after that moment. As the sample expands, the density in the sample falls to about 0.02 g/cm^3 at 2.0 ns after sample heating starts, with the density gradients in the sample decreasing to a level of no more than 25%.

IV. RESULTS AND DISCUSSION

Calculations of aluminum transmission have been carried out based on the LTE approximation. The aluminum K -shell absorption spectra that come from bound-bound absorption due to $1s-np$, $n=3,4,5,6$, transitions and from bound-free absorption were computed from the simulated temperature and density. In the calculations, the bound-bound absorption was calculated using the detailed-term-accounting opacity model code coupled to spectroscopically accurate atomic data generated by the COWAN code. The calculations include states from heliumlike through neonlike ionization sequences and levels with principal quantum number up to $n=6$ and orbital quantum number up to $l=3$. In addition to the ground and low-lying excitation configurations chosen by Abdallah [4], some low-lying excitation configurations as $1s^2 2s^1 2p^{m+1}$ were also included. The bound-free contribution was calculated from the average-atom model and was also added to the absorption. However, the free-free contribution to the absorption was neglected since it is a minor contribution to the total absorption in the measured wavelength range. Thus, the frequency-dependent absorption coefficients used in the present work are expressed as

$$\mu(\nu) = \frac{1}{\rho} \sum_i \left(\sum_{l'l''} N_{il} \sigma_{ill'}(\nu) + \sum_l N_{il} \sigma'_{il}(\nu) \right), \quad (7)$$

where $\sigma_{ill'}(\nu)$ represents the line absorption cross section from level l to level l' of an ion in the i th ionization degree,

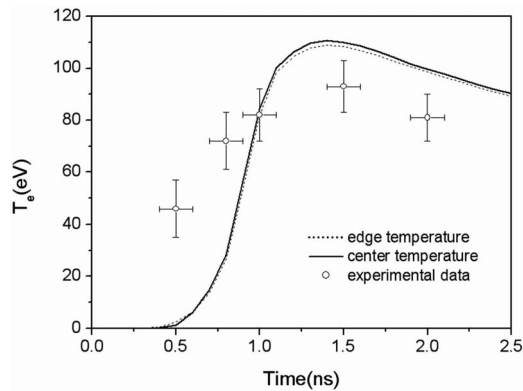


FIG. 6. (Color online) Measured and simulated temperatures in the aluminum foil. The calculations are given by the solid and dotted lines. The measured temperatures (circles) are time averaged over the backlight duration.

and $\sigma_{ill}(v)$ is the photoionization cross section from level l . N_{il} represents the ion density at level l .

It should be noted that in the calculations the densities in the sample were predicted from the hydrodynamics simulations, while the electron temperatures were varied to obtain the best fit of the experimental data. Plotted in Fig. 5 are the measured and calculated transmissions at the moment the backlight turns on, with the dashed lines representing the measured and the solid the calculated transmission. By fitting the experimental absorption spectra with theoretical calculations, the electron temperatures are obtained and shown in Fig. 6. The error bars on Fig. 6 represent the combined uncertainties from both the measurement errors (about 10%) and the temperature variations in the sample due to density variations in both space and time, with the temperature uncertainty related to uncertainty in the density being about 22% at 500 ps, 11% at 800 ps, 7% at 1000 ps, 2% at 1500 ps, and 2% at 2000 ps. In comparison, deviations of about 25% are observed between the measured temperatures and the simulations at times after 1 ns, and even greater deviations of more than 50% at earlier times, so it is clear that the temperature variations in the sample due to density variations are not enough to explain the discrepancies between the inferred temperatures and the simulated ones. Another possible source of discrepancies is preheating from the M -band emission of gold. The Au M -band x rays ($\sim 2-4$ keV), which constitute a significant component ($\sim 10\%$) of the hohlraum radiation source and are able to penetrate the 200 μm foam shields and the 1.5 μm CH layer covering the sample with approximately 80% transmission (2.5 keV), can preheat the sample efficiently, as has been observed and reported by several researchers [24–26]. In addition, the incorrect equation of state and opacity data and the limited set of configurations included in the theoretical calculations may also be responsible for the discrepancies between the inferred temperatures and the calculations. These have long been unsolved problems related to the simulations of hot dense plasmas.

In order to compare the experimental data with theoretical calculations that assume LTE, we also want the sample to be in LTE in an opacity experiment. The LTE condition imposes a strong constraint on the temperature and density in the plasma. For an optically thin sample plasma, as is usually required in an opacity experiment, to keep the plasma in LTE, the electron density of the sample must be sufficiently high to ensure that the deexcitation rates by electron-ion collision are far greater than those by radiative decay. From the simulated evolution of the density and temperature in the sample plasma shown in Fig. 4, it can be seen that by 2.0 ns after sample heating the density in the plasma falls to the order of 10^{-2} g/cm³, which corresponds to an electron density around 10^{21} /cm³. The electron density, together with the temperature of about 100 eV, gives a ratio of radiative to collisional rates of order 10^{-3} , which is low enough to ensure LTE in the sample.

V. CONCLUSIONS

We have proposed a compact hohlraum for opacity experiments and have carried out hydrodynamic simulations and experimental measurements of the temperature evolution in the radiatively heated sample. By point-projection spectrometry with a short-pulse backlight, the evolution of electron temperature in the heated sample was obtained by fitting the experimental aluminum transmissions with theoretical calculations, and a maximum temperature of about 93 eV was found in the aluminum sample. By comparing the experimental measurements with the simulated results, we find that the experiments conform to the simulations within 25% at times after 1 ns and we consider this an overall agreement between the measured temperatures and the theoretical simulations. The results prove that our proposal for a foam-buffered compact hohlraum is helpful in creating high temperatures in an opacity sample.

In summary, the compact hohlraum, together with the foam shields, has made it possible for us to utilize the laser energy more efficiently and create higher temperature in an opacity sample. We have not tried to measure the opacity data quantitatively in this work since our aim is mainly to test the target designs for opacity measurements at higher temperature with a relatively low laser energy. More quantitative measurements of the opacity using this type of target are planned, using a spatially resolved point-projection spectrometer with carefully calibrated spectrometer and films.

ACKNOWLEDGMENTS

This work was performed under the auspices of the National Natural Science Fund of China (Grant No. 10875109) and the Science and Technology Fund of CAEP (Grant No. 2007B08003). We also would like to thank the SG-II operation staff and the target preparation staff for cooperation.

- [1] F. J. Rogers and C. A. Iglesias, *Science* **263**, 50 (1994).
- [2] David P. Kilcrease, Los Alamos National Laboratory Report No. LA-UR-05-7470, 2005 (unpublished).
- [3] G. D. Tsakiris and K. Eidmann, *J. Quant. Spectrosc. Radiat. Transf.* **38**, 353 (1987).
- [4] J. Abdallah, Jr. and R. E. H. Clark, *J. Appl. Phys.* **69**, 23 (1991).
- [5] J. Bauche, C. Bauche-Arnoult, J.-F. Wyart, P. Duffy, and M. Klapisch, *Phys. Rev. A* **44**, 5707 (1991).
- [6] C. A. Back, T. S. Perry, D. R. Bach *et al.*, *J. Quant. Spectrosc. Radiat. Transf.* **58**, 415 (1997).
- [7] T. S. Perry, S. J. Davison, F. J. D. Serduke *et al.*, *Phys. Rev. Lett.* **67**, 3784 (1991).
- [8] T. S. Perry *et al.*, *J. Quant. Spectrosc. Radiat. Transf.* **54**, 317 (1995).
- [9] T. S. Perry, P. T. Springer, and D. F. Fields, *Phys. Rev. E* **54**, 5617 (1996).
- [10] T. S. Perry, R. I. Klein, D. R. Bach, K. S. Budil, R. Cauble, H. N. Kornblum, R. J. Wallace, and R. W. Lee, *Phys. Rev. E* **58**, 3739 (1998).
- [11] L. B. Da Silva, B. J. MacGowan, D. R. Kania, B. A. Hammel, C. A. Back, E. Hsieh, R. Doyas, C. A. Iglesias, F. J. Rogers, and R. W. Lee, *Phys. Rev. Lett.* **69**, 438 (1992).
- [12] P. T. Springer, D. J. Fields, B. G. Wilson *et al.*, *Phys. Rev. Lett.* **69**, 3735 (1992).
- [13] S. J. Davidson, J. M. Foster, C. C. Smith, K. A. Warburton, and S. J. Rose, *Appl. Phys. Lett.* **52**, 847 (1988).
- [14] C. Chenais-Popovics *et al.*, *J. Quant. Spectrosc. Radiat. Transf.* **71**, 249 (2001).
- [15] G. Winhart, K. Eidmann, C. A. Iglesias, and A. Bar-Shalom, *Phys. Rev. E* **53**, R1332 (1996).
- [16] J. Y. Zhang *et al.*, *Phys. Plasmas* **14**, 103301 (2007).
- [17] J. J. MacFarlane, J. E. Bailey, G. A. Chandler *et al.*, *Phys. Rev. E* **66**, 046416 (2002).
- [18] G. A. Rochau, J. E. Bailey, and J. J. MacFarlane, *Phys. Rev. E* **72**, 066405 (2005).
- [19] J. E. Bailey, G. A. Rochau, C. A. Iglesias *et al.*, *Phys. Rev. Lett.* **99**, 265002 (2007).
- [20] Y. Xu *et al.*, *Phys. Plasmas* **14**, 052701 (2007).
- [21] J. Edwards *et al.*, *Phys. Plasmas* **7**, 2099 (2000).
- [22] G. Gregori, S. H. Glenzer, K. B. Fournier, K. M. Campbell, E. L. Dewald, O. S. Jones, J. H. Hammer, S. B. Hansen, R. J. Wallace, and O. L. Landen, *Phys. Rev. Lett.* **101**, 045003 (2008).
- [23] C. A. Back, J. D. Bauer, O. L. Landen, R. E. Turner, B. F. Lasinski, J. H. Hammer, M. D. Rosen, L. J. Suter, and W. H. Hsing, *Phys. Rev. Lett.* **84**, 274 (2000).
- [24] E. L. Dewald *et al.*, *Phys. Plasmas* **15**, 072706 (2008).
- [25] R. F. Smith, S. M. Pollaine, S. J. Moon, K. T. Lorenz, P. M. Celliers, J. H. Eggert, H. S. Park, and G. W. Collins, *Phys. Plasmas* **14**, 057105 (2007).
- [26] D. C. Swift, T. E. Tierney, S. N. Luo, D. L. Paisley, G. A. Kyrala, A. Hauer, S. R. Greenfield, A. C. Koskelo, K. J. McClellan, H. E. Lorenzana, D. Kalantar, B. A. Remington, P. Peralta, and E. Loomis, *Phys. Plasmas* **12**, 056308 (2005).